

Accepted Manuscript

Title: Oxidative Dehydrogenation of Ethyl Lactate over Nanocarbon Catalysts: Effect of Oxygen Functionalities and Defects

Authors: Dan Wang, Wei Liu, Zilai Xie, Siyuan Tian, Dangsheng Su, Wei Qi



PII: S0920-5861(18)30742-9
DOI: <https://doi.org/10.1016/j.cattod.2018.06.018>
Reference: CATTOD 11507

To appear in: *Catalysis Today*

Received date: 27-2-2018
Revised date: 22-5-2018
Accepted date: 14-6-2018

Please cite this article as: Wang D, Liu W, Xie Z, Tian S, Su D, Qi W, Oxidative Dehydrogenation of Ethyl Lactate over Nanocarbon Catalysts: Effect of Oxygen Functionalities and Defects, *Catalysis Today* (2018), <https://doi.org/10.1016/j.cattod.2018.06.018>

This is a PDF file of an unedited manuscript that has been accepted for publication. As a service to our customers we are providing this early version of the manuscript. The manuscript will undergo copyediting, typesetting, and review of the resulting proof before it is published in its final form. Please note that during the production process errors may be discovered which could affect the content, and all legal disclaimers that apply to the journal pertain.

Oxidative Dehydrogenation of Ethyl Lactate over Nanocarbon Catalysts: Effect of Oxygen Functionalities and Defects

Dan Wang^{a,#}, Wei Liu^{b,#}, Zailai Xie^c, Siyuan Tian^b, Dangsheng Su^b, Wei Qi^{a,b,*}

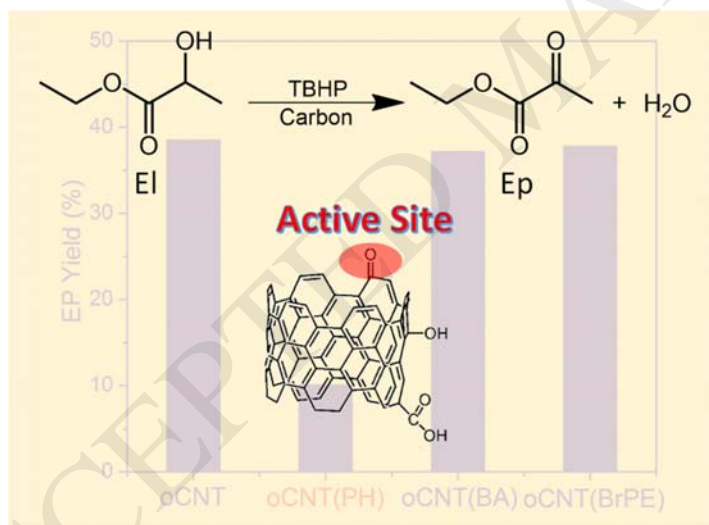
These authors contributed equally.

a. College of Sciences, Northeastern University, Shenyang, Liaoning, 110819, China.

b. Shenyang National Laboratory for Materials Science, Institute of Metal Research, Chinese Academy of Sciences, Shenyang, Liaoning, 110016, China, Email: wqi@imr.ac.cn

c. State Key Laboratory of Photocatalysis on Energy and Environment, College of Chemistry, Fuzhou University, Fuzhou, Fujian, 350002, China.

Graphical Abstract



Highlights

- Green chemical synthesis of ethyl pyruvate.
- Nanocarbon materials catalyze oxidative dehydrogenation of ethyl lactate.
- Active site identification via chemical titration method.
- Structural evolution of carbon catalysts during oxidative dehydrogenation reactions.

- Reaction mechanism for carbon catalyzed liquid-phase reactions revealed via multiple in situ characterization methods.

Abstract

Pyruvic acid and pyruvate derivatives are important chemical intermediates which are normally produced using metal-based catalytic materials that could cause serious environmental problems. In the present work, renewable nanocarbon catalysts are applied in this system, and a solvent free and highly selective oxidative dehydrogenation of ethyl lactate (EL) process is achieved to produce ethyl pyruvate (EP) under mild reaction conditions. Chemical titration results provide direct evidence that ketonic carbonyl groups on nanocarbon are active sites for this reaction. Raman, XPS and model catalyst experimental results have shown that there is a dynamic transformation between defects and oxygen functionalities during the catalytic reactions. The reaction pathway is revealed via kinetic analysis, which may shed light on the rational design of carbon catalysts and their potential catalytic applications in the field of fine chemical productions.

Keywords: Heterogeneous catalysis; Carbon catalysis; Oxidative dehydrogenation; O-H bond activation; Active site.

1. Introduction

Pyruvic acid and pyruvate derivatives are important chemical intermediates for the large scale production of wine additives, perfumes, cosmetics, pesticides and medicines [1-4]. Pyruvic acid is conventionally produced via dehydrative decarboxylation reaction of tartaric acid [5], and the major disadvantage of this synthetic route is the requirement of excess KHSO_4 as dehydration agent, leading to a high cost, low atomic efficiency and environmentally detrimental process [5-6]. Oxidative dehydrogenation (ODH) is one of the most promising strategy to replace the dehydrative decarboxylation method producing lactic acid/ester compounds, such

as the selective catalytic conversion of ethyl lactate (EL) to ethyl pyruvate (EP) [7]. In this process, the reactant EL could be obtained from biomass, which is considered as renewable green chemicals [8-10]. The reaction does not lose carbon and only produces EP and H₂O as products, exhibiting relatively high atomic efficiency and sustainability. The ODH pathway has shown great potential for the eco-friendly production of highly valued pyruvate products using renewable carbohydrate feed stocks [11].

The current existing catalysts for the ODH of pyruvate are almost all metal-based compounds, such as mixed oxides (MoO₃ etc.), Mo-doped iron phosphate, MoVNbO_x catalysts for gas phase and heteroatom doped-Pd/C for liquid phase pyruvate ODH processes etc. [2]. One irreconcilable drawback of these metal-based catalysts is the relatively limited resources and inevitable environmental issues that could not meet the extremely high requirement for modern green and sustainable chemistry. Developing novel renewable and efficient catalysts is essentially important in realizing the industrial potential for pyruvate ODH reactions [12].

Aiming at these challenges, we pay our attention to the emerging nanocarbon catalysis, where low-cost, earth abundant and renewable nanocarbon materials have already proven their efficiency for the reactions involving C-H bond activations (dehydrogenation of aromatic or chain alkanes) [13-14] and O-H bond activation [15]. In this work, we report the first direct use of oxidized multi-wall carbon nanotube (oCNT) as efficient catalysts for the highly selective synthesis of EP via EL ODH, showing that nanocarbon is also active in the activation of O-H bonds. The catalytic reactions were conducted under solvent free and atmospheric pressure conditions, which is a gentle, green and energy-saving process. Mechanistic studies indicate that the surface oxygen functional group is responsible for the activity of nanocarbon, and ketonic carbonyl groups are further identified as the main active sites using chemical titration method and XPS analysis. Raman spectrum and model catalyst experiments reveal that surface reconstruction during reaction is also vital to the activity and stability of the nanocarbon catalysts.

2. Experimental section

2.1 Materials

Pristine multiwall carbon nanotubes (pCNT) were supplied by Shandong Dazhan Nano-materials Co., Ltd (China). Ultra-dispersed diamond (UDD) were purchased from Sigma-Aldrich. Activated carbon materials were purchased from Sinopharm. Ethyl lactate (EL), phenylhydrazine (PH), benzoic anhydride (BA) and 2-bromo-1-phenylethanone (BrPE) was purchased from Alfa Aesar.

2.2 Synthesis of the catalysts

Oxidized CNT (oCNT) was obtained via HNO_3 oxidation of pristine multiwall carbon nanotubes (pCNT). In a typical process, pCNT (1 g) was oxidized in concentrated HNO_3 (68%) under reflux at 120 °C for 2h. The precipitate was filtered out and washed to neutral with deionized water. The precipitate was dried in vacuum at 120 °C for 24 h to give black oxidized carbon nanotubes (oCNT). Oxidized carbon nanotubes with defects (oCNT-d) was prepared by heating oCNT at 925 °C in Ar for 2 h. Graphite oxide and graphene oxide catalyst were kindly supplied by Sinocarbon Co. (Institute of Coal Chemistry, Chinese Academy of Sciences) and donated as G1, G2 respectively.

The oxidized onion like carbon (oOLC) was prepared as following procedures. First, ultra-dispersed diamond (UDD) was heated at 1300 °C in argon atmosphere for 6 h to obtain OLC. Then, OLC (1 g) was collected and refluxed in 100 mL HNO_3 (68%) at 120 °C for 2 h. The resulting oxidized OLC, labelled as oOLC, was filtered and washed with deionized water until the pH of the filtrate reached neutral and then dried at 120 °C overnight.

2.3 Chemical titration of the active sites

The titration of the ketonic carbonyl groups on oCNTs was performed as following procedures. Phenylhydrazine (PH, 99%, 2 g) and small amount of HCl acid (38 %, 100 μL) was dissolved in CHCl_3 (100 ml), and then oCNT (1 g) was added into the solution. After stirring under N_2 protection for 72 h, the precipitate was filtered out and washed with CHCl_3 in Soxhlet extractor for 20 h to remove the

physical adsorbed PH molecules. The precipitate was dried in vacuum at 60 °C for 24 h to give black carbon nanotube titration derivatives (oCNT(PH)).

The titration of phenol groups on oCNTs was performed as following procedures. Benzoic anhydride (BA, 98 %, 5 g) and oCNT (1 g) was dissolved in CHCl₃ (50 ml). After stirring under N₂ protection at 60 °C for 24 h, the precipitate was filtered out and washed with CHCl₃ to remove the physical adsorbed BA molecules. The precipitate was dried in vacuum at 60 °C for 24 h to give black carbon nanotube titration derivatives (oCNT(BA)).

The titration of carboxylic acid groups on oCNTs was performed as following procedure. 2-bromo-1-phenylethanone (BrPE, 99%, 2 g) and oCNT (1 g) was dissolved in CHCl₃ (50 ml). After stirring under N₂ protection at room temperature in dark for 5 h, the precipitate was filtered out and washed with CHCl₃ to remove the physical adsorbed BrPE molecules. The precipitate was dried in vacuum at 60 °C for 24 h to give black carbon nanotube titration derivatives (oCNT(BrPE)).

Control titration experiments were performed using small molecules of phenol (-OH), benzoic acid (-COOH) and benzophenone (-C=O), respectively, following the similar procedure as above (r.t. in 50 mL CHCl₃). The molar ratio between the molecular substrates and the titrants were controlled at 1:50.

2.4 Catalytic reactions

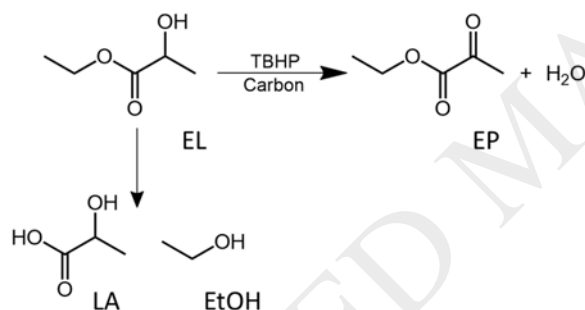
Typically, the catalytic EL ODH reaction was performed as following procedures. EL (0.59 g, 5 mmol) and catalysts (50 mg) were dispersed in t-butylhydroperoxide (TBHP, 65%, 2.7 g, 20 mmol) in a flask equipped with a reflux condenser under atmospheric pressure, and the reaction mixture was stirred at 300 rpm at 90 °C for 6 h. After reaction, the catalyst was filtered out and the filtrates were diluted to 25 mL for further analysis. The products were analysed using an Agilent 7890 gas chromatography system with HP-5 column and a flame ionization detector (FID).

2.5 Characterizations

XPS spectra were obtained by using a surface analysis system (ESCALAB 250, Thermo VG, USA) with Al K_α X-rays (1486.6 eV, 150 W, 50.0 eV pass energy). The

O1s XPS spectra were fitted using mixed Gaussian-Lorentzian component profiles (at a ratio of 80/20) after subtraction of a Shirley background using XPSPEAK41 software. The fitting was performed by fixing the peak position for individual species within 0.05 eV and applying a full width at half-maximum (FWHM) of 1.2-1.6 eV. Raman spectroscopies were recorded with a LabRam HR 800 using 532 nm laser. Transmission electron microscopy (TEM) images were recorded on a FEI Tecnai T12 with an accelerating voltage of 120 kV. Attenuated total reflectance (ATR) FTIR spectra were recorded using a Varian spectrometer equipped with a liquid-nitrogen cooled mercury cadmium telluride (MCT) detector. Spectra were recorded at 4 cm⁻¹ resolution in the region of 4000–550 cm⁻¹.

3. Results and discussion



Scheme. 1. EL conversion routes on carbon catalysts.

Firstly, we tested the EL ODH catalytic performance of various carbon materials, including conventional amorphous activated carbon (powdered activated carbon (pAC), granular activated carbon (gAC)) and some typical nanocarbon materials (CNT, Graphite Oxide (G1), Graphene Oxide (G2) and oxidized onion-like carbon (oOLC)) etc. The key structural parameters, including shape, size, surface area and oxygen content etc., for these carbon materials are listed in Table S1, and the overall catalytic performance of these carbon materials in EL ODH reactions are shown in Table 1. The reaction was performed under very gentle reaction conditions (90 °C, ambient pressure, without solvent). EP, ethanol and lactic acid are the only detected products indicating dehydrogenation (EP as product) and hydrolysis (side reaction

with ethanol and lactic acid as products) are the main reaction routes under the chosen conditions as shown in Scheme 1.

The yield of EP is below 4.8 % in the absence of the catalysts at the selectivity of 39.6 (see blank test in Table 1). The introduction of carbon catalysts could obviously enhance the oxidative dehydrogenation reaction. In general, nanocarbons exhibit higher activity (EL conversion) than amorphous active carbon (pAC and gAC). However, only carbon nanotube (CNT) materials exhibit relatively high EP selectivity (over 90%), while the EP selectivity on graphite oxide and graphene oxide catalysts is below 15 %. GC analysis shows that the main side reaction is the hydrolysis of EL or EP. It is generally accepted that graphite oxide related materials contain a lot of oxygen functional groups, and the majority of them are carboxylic acid groups [16-18]. Therefore, the poor selectivity of graphite oxide and graphene oxide may be attributed to the presence of excess acidic carboxylic acid group on their surface leading to drastic hydrolysis reactions. Although pAC and gAC exhibit acceptable selectivity to EP (around 98%), their EL conversion is obviously lower than oCNT catalysts. Among all carbon materials, oCNT and SWCNT exhibit the best performance. The superiority of SWCNT over oCNT might originate from its larger specific surface area (425 vs. 219 m²/g). It is worthy to point out that the oOLC catalysts, which usually exhibit superior activity over CNT in alkane ODH reactions [19], exhibits poor activity in both selectivity and conversion. Oxygen could also be used as oxidant for the ODH reactions, and oCNT catalysts exhibit the EP yield at 16.9 % in a fixed bed reactor at 260 °C (2 kPa EL, 1kPa O₂, balanced He, ambient pressure). In summary, Table 1 clearly demonstrates that carbon materials, especially nanocarbons (such as CNTs), could be used as catalysts for catalytic dehydrogenation of EL to produce EP.

Table 1. Summary of the activity of carbon catalysts in EL ODH reaction.^a

Sample	Catalytic performance/%		
	Conversion ^b	Selectivity ^c	Yield ^c

Blank	12.1	39.6	4.8
oCNT	39.0	93.6	36.5
oCNT ^d	47.0	36.0	16.9
SWCNT	41.1	98.5	40.5
oOLC	25.5	60.6	15.5
G1	43.6	13.6	5.9
G2	67.4	6.9	4.7
pAC	29.5	98.5	29.1
gAC	23.4	98.5	23.1

a, reaction condition: 0.59g EL, 2.7g TBHP, 50 mg carbon catalyst, 90 °C, 6h;

b, conversion of EL;

c, selectivity and yield of EP

d, O₂ as oxidant in fixed bed reactor, reaction conditions: 2 kPa EL, 1kPa O₂, balanced He, 100 mg oCNT, 260 °C.

The reusability test (as shown in Fig. S1) shows that the activity (EL conversion) and selectivity (for EP) of oCNT catalysts are well maintained in the second run, but the recovered activated carbon (both pAC and gAC) catalysts exhibit obvious conversion and selectivity drop during the reuse process. The main reason for the distinct reusability of these two types of carbon catalysts should be attributed to their different degree of order, namely the conjugation size of carbon skeleton. Activated carbon catalysts may lose active sites after filtration, since the small carbon fragments with less conjugation size may leach into liquid phase [20]. On the contrast, CNT catalysts with relatively high degree of order (well-organized sp² conjugated graphitic carbon framework) ensure their structural stability and superior reusability in the reaction. In general, oCNT is chosen as the best candidate carbon catalyst for EL ODH reaction, which exhibits favourable activity and reusability over traditional activated carbon materials.

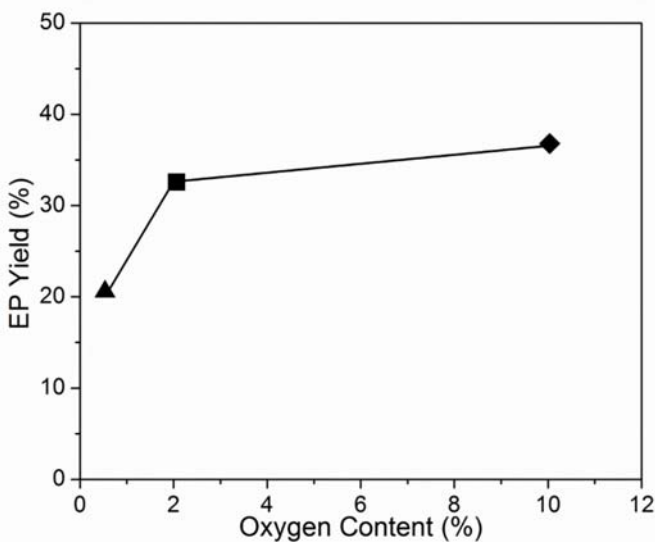


Fig. 1. EP yield as a function of oxygen content in oCNT-d (triangle), pCNT (square) and oCNT (diamond).

Understandings on active sites is the foundation for the mechanistic studies on catalytic reactions. Oxygen functionalities play a vital role in carbon catalysed redox reactions [21], which is firmly confirmed in gas-phase alkane ODH reactions, such as ODH of ethylbenzene and propane etc. [22-24]. To examine the role of oxygen functional groups in catalysis, we prepared three CNT samples that have similar structure but different surface oxygen content (denoted as oCNT, pCNT and oCNT-d with oxygen content at 10.1, 2.0 and 0.6 %, respectively, as shown in Table S1). As shown in Fig. 1, the EL ODH catalytic activity of the CNT samples increases with surface oxygen content, indicating that surface oxygen functionalities may be responsible for the catalytic activity, but the non-linear dependence suggest that maybe not all of the oxygen groups are active on EL ODH reactions. Identification of the active sites remain full of challenges because of the complexity of nanocarbon surface functionalities, such as the coexistence of ketonic carbonyl, carboxyl and hydroxyl groups etc.

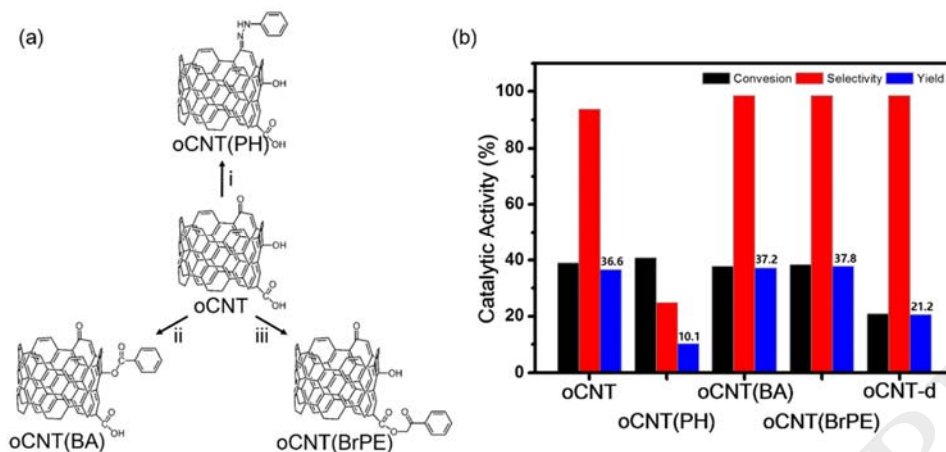


Fig. 2. (a) Titration process for (i) ketonic carbonyl, (ii) phenol and (iii) carboxylic acid groups on nanocarbon; (b) EL ODH conversion, EP selectivity and yield on oCNT, oCNT titration derivatives and CNTs with only defects.

To identify and quantify the active sites for the reaction, we have proposed a chemical titration technique [25]. As shown in Fig. 2a, phenylhydrazine (PH), benzoic anhydride (BA) and 2-bromo-1-phenylethanone (BrPE) are applied as titrants. Control experiments using small organic substrates (benzophenone (-C=O), phenol (-OH), and benzoic acid (-COOH)) indicated that the titrants could selectively react with the ketonic carbonyl, hydroxyl and carboxylic groups on oCNT samples, respectively, and these three types of groups involve over 90 % of oxygen functionalities in total [26-27]. For example, PH molecules would react with ketonic carbonyl groups on nanocarbon forming hydrazone compounds at a yield over 99 % [25]. The role of specific oxygen functionalities could be revealed via comparing the catalytic performance of these titration derivatives (oCNT(PH), oCNT(BA) and oCNT(BrPE)). As shown in Fig. 2b, the EL ODH catalytic activity of oCNT(PH) is much lower (80 % lower) than that of oCNT, while oCNT(BA) and oCNT(BrPE) exhibit almost identical activity as oCNT, providing firm chemical evidence that ketonic carbonyl group is the active site for EL ODH reactions. It needs to be mentioned that the selectivity of oCNT(BA), oCNT(BrPE) towards EP are both over 95%, higher than that of oCNT (93.6%), indicating that the removal of hydroxyl or carboxylic acid groups could inhibit the side reactions, although they have shown negligible influence

on ODH activity.

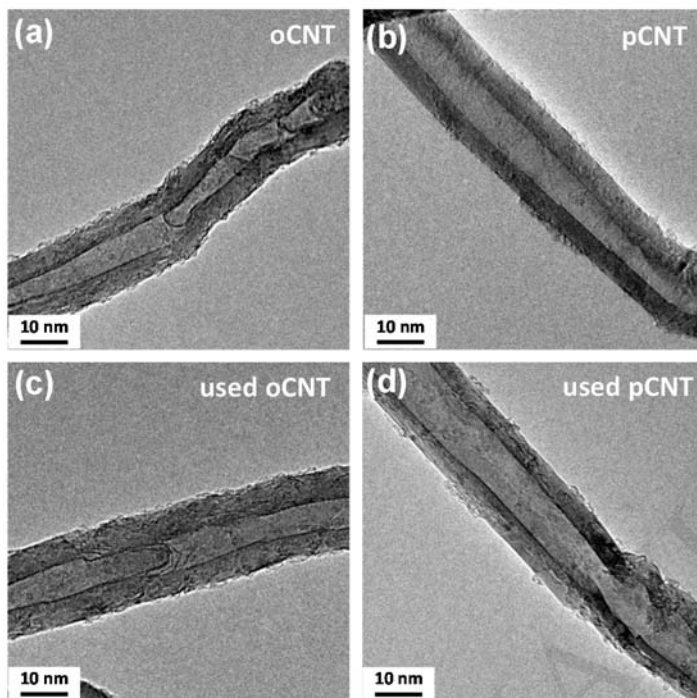


Fig. 3. TEM images of (a) oCNT, (b) pCNT, (c) used oCNT and (d) used pCNT.

The morphology, chemical composition and structure of nanocarbon catalysts before and after ODH reactions were revealed via TEM, XPS and Raman measurements. As shown in Fig. 3, TEM images of fresh and used CNT catalysts demonstrate that there is no obvious change in the general structure of carbon catalysts, suggesting that the bulk sp^2 structure is well-maintained during catalysis. However, the chemical composition of carbon catalysts may change under redox reaction conditions. For example, we observed that the oxygen content of untreated pristine CNT (pCNT) catalysts would increase (from 2.0 to 2.7 % as shown in Table 2) after one catalytic cycle, and especially the surface content of ketonic carbonyl groups doubled (from 0.3 to 0.7 %) during this process. This is also the possible reason why pCNT exhibits similar EL ODH catalytic activity as oCNT (EL conversion at 33 vs. 39 %), since they have similar surface content of ketonic carbonyl groups (0.7 vs. 1.0 %) after reaction, which is consistent with titration results that ketonic carbonyl groups are the active sites for EL ODH reactions.

Table 2. Summary of Raman and XPS analysis results on fresh and used CNT catalysts.^a

Sample	Raman peak percentage (%)					Element content from XPS (%)			
	1200 (D ₄)	1350 (D ₁)	1500 (D ₃)	1580 (G)	1620 (D ₂)	I _D /I _G	C	O	-C=O ^b
pCNT	9.5	47.8	6.1	29.1	7.5	1.6	98.0	2.0	0.3
used-pCNT	15.6	44.6	3.7	30.4	5.7	1.5	97.3	2.7	0.7
oCNT	13.5	44.8	7.0	28.2	6.5	1.6	96.2	3.8	1.0
used-oCNT	12.1	47.2	6.3	27.8	6.5	1.7	95.8	3.6	1.0

^a reaction condition: 0.59g EL, 2.7g TBHP, 50 mg carbon catalyst, 90 °C, 6h;

^b surface content of ketonic carbonyl groups from deconvolution of O 1s XPS (as shown in Fig. S2).

Raman spectroscopy is an effective method to reveal the surface structure change of nanocarbon materials. The overall shapes of Raman spectra for fresh and used CNT catalysts are similar, which is consistent with the TEM measurements that the structural integrity of the CNTs is well reserved during the reaction. The Raman spectrum for carbon materials could be deconvoluted into five peaks corresponding to ideal graphitic lattice (G, ~1580 cm⁻¹), disordered graphitic lattice (graphene layer edges, D₁, ~1350 cm⁻¹), disordered graphitic lattice (surface graphene layers, D₂, ~1620 cm⁻¹), amorphous carbon (D₃, ~1500 cm⁻¹) and disordered graphitic lattice (polyenes, ionic impurities, D₄, ~1200 cm⁻¹) [28]. I_D/I_G is defined as the intensity ratio of D₁ and G band, which is normally used to quantify the surface content of defects (namely the degree of graphitization) for carbon materials [29-30]. As shown in Table 2 (summary of the Raman peak and XPS deconvolution results), the value of I_D/I_G for pCNT slightly decreases (1.6 to 1.5), and the oxygen content increases (2.0 % to 2.7 %), indicating that there may be a transformation from defects to oxygen functionalities (mainly ketonic carbonyl groups) during the catalytic reactions. On the contrast, oCNT catalysts exhibit the opposite trend (I_D/I_G increases from 1.6 to 1.7, oxygen content decreases from 3.8 % to 3.6 % after reaction) suggesting the possible

transformation from oxygen functionalities to defects. This phenomenon clearly shows the dynamic change of the carbon surface structure, namely the transformation between defects and various oxygen functionalities, during the catalytic reaction process. This surface reconstruction phenomenon is also observed in carbon catalyzed gas phase reactions [19], and it has significant influence on the activity and stability of carbon catalytic materials, which also emphasizes the importance for considering the chemical structure of carbon catalysts under reaction conditions.

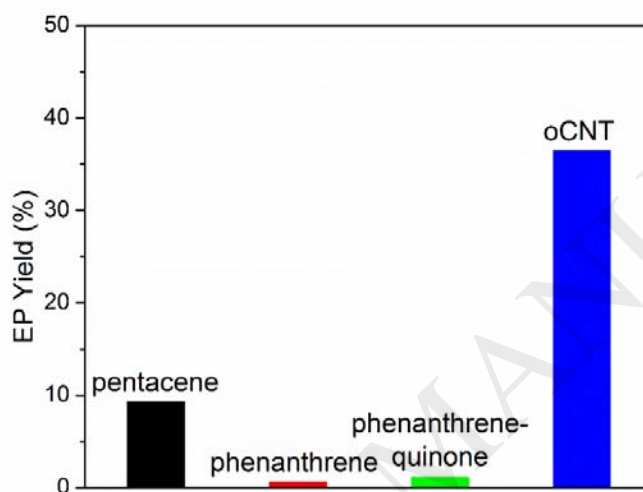


Fig. 4. EL ODH activity (EP yield) on pentacene, phenanthrene, phenanthrenequinone and oCNT.

Small organic molecules are also used as model catalysts to testify the hypothesis on the active sites and the dynamic structure change during catalysis. As shown in Fig. 4, phenanthrene, pentacene and phenanthrenequinone, presenting armchair and zigzag type of defect and ketonic carbonyl groups respectively, are chosen as model catalysts running EL ODH under the same reaction conditions as CNT materials. As shown in Fig. 4, pentacene have shown much higher activity than phenanthrene catalysts (conversion at 9.3 % vs. 0.6 %) in EL ODH reactions, indicating that Zigzag type defect would be more active than armchair. Attenuated Total Reflection Fourier Transform IR (ATR-FTIR) spectrum of the used pentacene catalysts showed that ketonic carbonyl groups are *in situ* generated on the molecules during the catalytic reactions (1680 cm^{-1} , stretching vibration band of C=O structure, Fig. S3). The

observation indicates that Zigzag defect could be converted into ketonic carbonyl groups during the catalytic reaction, which is consistent with the experimental observations on pCNT catalysts that the surface content of ketonic carbonyl groups increased after EL ODH reactions. It seems abnormal that phenanthrenequinone compounds exhibits relatively low ODH activity, since they contain abundant ketonic carbonyl groups in their structure. Actually, ATR-IR measurements on fresh and used phenanthrenequinone samples exhibit that most of the ketonic carbonyl groups decomposed after catalytic EL ODH reaction (C=O stretching vibration band at 1680 cm^{-1} dramatically shrinks as shown in Fig. S3). The observation suggests that unstable C=O groups would be decomposed during the catalytic reactions, which is just similar as that the oxygen content on oCNT catalysts decreases after ODH reactions. The catalytic activity test and structure analysis on model small-molecular catalysts have proven that ketonic carbonyl groups serve as the active sites for EL ODH reactions, and there is a transformation between defects (mainly Zigzag type) and ketonic carbonyl groups. This transformation depends on the initial structure of the carbon catalysts and also the employed reaction conditions. Comparing with nanocarbon, the lower catalytic activity of small organic molecules might be related to their less conjugation size. The relatively large conjugated sp^2 structure of nanocarbon ensure the good catalytic activity and stability in ODH reactions.

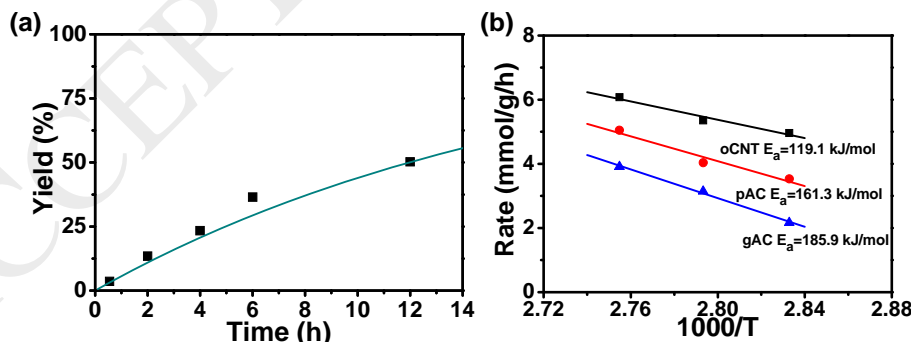
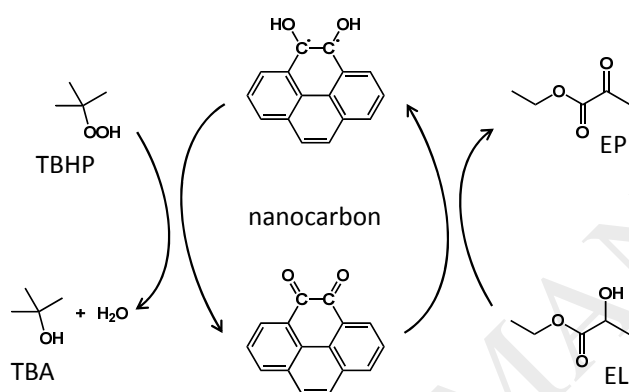


Fig. 5. (a) EP yield as a function of reaction time for EL ODH reaction under the catalysis of oCNT. (b) Apparent activation energy for oCNT, pAC and gAC according to Arrhenius equation in EL ODH reaction. Reaction condition: 0.59g EL, 2.7g TBHP, 50 mg carbon catalyst, 90 °C.

The EL ODH reactions follow pseudo-first order reaction kinetics under the catalysis of oCNTs as shown in Fig. 5a, and the measured first order rate constant k equals to 0.058 S^{-1} . The activation energy could be derived from the dependence of ODH reaction rates on reaction temperature via Arrhenius equation as shown in Fig. 5b. oCNT catalysts exhibit lower activation energy than activated carbon materials (119.1 vs. 161.3 and 185.9 kJ/mol), indicating the long ranged ordered graphitic structure may benefit the ODH reactivity [21], which is consistent with the observations on model organic molecular catalysts.



Scheme 2. Proposed reaction pathway for EL ODH on nanocarbon catalysts (the backbone of nanocarbon is simplified as four benzene rings).

Combing the active site titration, structural evolution measurements, model catalysts and kinetic analysis results, we propose a reaction mechanism for carbon catalyzed EL ODH reactions as shown in Scheme 2. The reactants EL molecules may first adsorb on ketonic carbonyl groups on carbon surface. The products EP form and desorb after the sequential hydrogen abstraction processes, and the carbon catalysts get reduced (forming hydroxyl groups) during this process. Finally, the reduced carbon catalysts are re-oxidized by TBHP to complete the reaction cycle. In this step, some unstable hydroxyl groups could be decomposed forming defects or disordered carbon atoms. It should be mentioned that Scheme 2 only summarizes the possible reaction pathway but not the exact reaction mechanism for carbon catalyzed EL ODH process under molecular level. The details for the reaction mechanism (such as the activation of molecular oxygen etc.) could be achieved via *in situ* spectroscopic

analysis.

4. Conclusions

In summary, a solvent free, highly selective ODH conversion route from EL to EP has been developed via green non-metallic nanocarbon catalysis. oCNT exhibit higher selectivity than graphene oxides and onion like carbon catalysts and better reusability than traditional activated carbon materials. Chemical titrations provide direct chemical evidence that ketonic carbonyl groups serve as the active sites for this reaction. Raman, XPS and model catalyst experimental results have shown that there is a dynamic transformation between defects and oxygen functionalities during the catalytic reactions. The direction of this transformation depends on the initial structure of the carbon catalysts and also the reaction conditions. Kinetic analysis shows that carbon catalyzed EL ODH is a pseudo first order reaction with an activation energy at about 119.1 kJ/mol. The relative high activity of oCNTs provides us a potential alternative metal-free system for the large scale production of ethyl pyruvate, which might be enlightened for related industry to meet the requirements of green and sustainable chemistry.

Acknowledgements

The authors acknowledge financial support from the NSFC of China (21761132010, 91645114, and 21573256) and the Youth Innovation Promotion Association, CAS.

References

- [1] T. Yasukawa, W. Ninomiya, K. Ooyachi, N. Aoki, K. Mae, *Chem. Eng. J.* 167 (2011) 527-530.
- [2] X. Zhao, C. Zhang, C. Xu, H. Li, H. Huang, L. Song, X. Li, *Chem. Eng. J.* 296 (2016) 217-224.
- [3] A. Corma, S. Iborra, A. Velty, *Chem. Rev.* 107 (2007) 2411-2502.
- [4] T. Furumoto, T. Yamaguchi, Y. Ohshima-Ichie, M. Nakamura, Y. Tsuchida-Iwata, M. Shimamura, J. Ohnishi, S. Hata, U. Gowik, P. Westhoff, A. Brautigam, A. P.

- Weber, K. Izui, *Nature* 476 (2011) 472-475.
- [5] S. Sugiyama, *J. Catal.* 129 (1991) 12-18.
- [6] E. V. Ramos-Fernandez, N. J. Geels, N. R. Shiju, G. Rothenberg, *Green Chem.* 16 (2014) 3358.
- [7] H. Hayashi, N. Shigemoto, S. Sugiyama, N. Masaoka, K. Saitoh, *Catal. Lett.* 19 (1993) 273-277.
- [8] B. Katryniok, S. Paul, F. Dumeignil, *Green Chem.* 12 (2010) 1910.
- [9] M. Dusselier, P. Van Wouwe, A. Dewaele, E. Makshina, B. F. Sels, *Energ. Environ. Sci.* 6 (2013) 1415.
- [10] M. Ai, K. Ohdan, *Applied Catalysis A: General* 150 (1997) 13-20.
- [11] T. J. Schwartz, B. J. O'Neill, B. H. Shanks, J. A. Dumesic, *ACS Catal.* 4 (2014) 2060-2069.
- [12] W. Qi, P. Yan, D. S. Su, *Acc. Chem. Res.* 51 (2018) 640-648.
- [13] W. Liu, B. Chen, X. Duan, K-H Wu, W. Qi, X. Guo, B. Zhang, D. Su, *ACS Catal.* 7 (2017) 5820-5827.
- [14] L. Shi, W. Qi, W. Liu, P. Yan, F. Li, J. Sun, D. S. Su, *Catal. Today* 301 (2018) 48-54.
- [15] N. Keller, N. I. Maksimova, V. V. Roddatis, M. Schur, G. Mestl, Y. V. Butenko, V. L. Kuznetsov, R. Schlögl, *Angew. Chem. Int. Ed.* 41 (2002) 1885.
- [16] G. Eda, M. Chhowalla, *Adv. Mater.* 22 (2010) 2392-2415.
- [17] S. Tang, W. Wu, L. Liu, Z. Cao, X. We, Z. Chen, *Phys. Chem. Chem. Phys.* 19 (2017) 11142-11151.
- [18] O. C. Compton, S. T. Nguyen, *Small* 6 (2010) 711-723.
- [19] W. Qi, W. Liu, X. Guo, R. Schlögl, D. Su, *Angew. Chem. Int. Ed.* 54 (2015) 13682-13685.
- [20] W. Liu, W. Qi, X. Guo, D. S. Su, *Chem. Asia. J.* 11 (2016) 491-497.
- [21] X. Guo, W. Qi, W. Liu, P. Yan, F. Li, C. Liang, D. S. Su, *ACS Catal.* 7 (2017) 1424-1427.
- [22] R. Schlögl, *Angew. Chem. Int. Ed.* 54 (2015) 3465-3520.
- [23] W. Qi, D. S. Su, *ACS Catal.* 4 (2014) 3212-3218.
- [24] X. Sun, Y. Ding, B. Zhang, R. Huang, D. Chen, D. S. Su, *ACS Catal.* 5 (2015)

2436-2444.

- [25] W. Qi, W. Liu, B. Zhang, X. Gu, X. Guo, D. Su, *Angew. Chem. Int. Ed.*, 52 (2013) 14224-14228.
- [26] I. Gerber, M. Oubenali, R. Bacsa, J. Durand, A. Goncalves, M. F. Pereira, F. Jolibois, L. Perrin, R. Poteau, P. Serp, *Chem. Euro. J.* 17 (2011) 11467-11477.
- [27] S. Kundu, Y. Wang, W. Xia, M. Muhler, *J. Phys. Chem. C* 112 (2008) 16869-16878.
- [28] A. Sadezky, H. Muckenhuber, H. Grothe, R. Niessner, U. Pöschl, *Carbon* 43 (2005) 1731-1742.
- [29] R. Wang, X. Sun, B. Zhang, X. Sun, D. Su, *Chem. Euro. J* 20 (2014) 6324-6331.
- [30] W. Xia, D. S. Su, A. Birkner, L. Ruppel, Y. M. Wang, C. Woll, J. Qian, C. H. Liang, G. Marginean, W. Brandl, M. Muhler, *Chem. Mater.* 17 (2005) 5737-5742.